The 15th International Symposium on Magnetic Bearings, August 3-6, 2016, Mojiko Hotel, Kitakyushu, Japan

ISMB15

Robust controller design for AMB levitation recovery

Alexander H. PESCH*, and Jerzy T. SAWICKI**

*Department of Engineering, Hofstra University

Hempstead, NY, USA

E-mail: alexander.h.pesch@hofstra.edu

**The Center for Rotating Machinery Dynamics and Control

Department of Mechanical Engineering, Cleveland State University

Cleveland, OH, USA

Abstract

A control method is proposed for relevitating an active magnetic bearing (AMB) system which has lost levitation due to an acute external fault. The proposed method involves switching to a robust recovery AMB controller once a delevitating event has been detected. The novel recovery controller is uniquely designed for levitation recovery using the robust control strategy μ-synthesis with performance weights which bound the disturbance force of the touchdown (TD) bearing on the rotor. Also, in contrast to typical AMB controller design, the recovery controller is designed to allow potential deflection up to the distance of the TD bearings so as to mitigate amplifier saturation during recovery.

The proposed method is demonstrated on an AMB test rig. Details on recovery controller design for the test rig are presented. Rotor drop tests are first used to tune a simple TD bearing model. Then, a numerical simulation is performed to find the frequency response of the TD bearing force on the rotor. The simulated frequency response is used to craft a force bounding performance weight which is then used for robust controller synthesis. The experimental rotor is run at 2000 RPM and a fault is induced by stopping current flow to the AMB coils. After approximately 2 s running on the TD bearings, the power is restored. When no recovery scheme is used, the rotor responds violently, hitting the top of the TD bearing before recovering levitation. With the proposed recovery scheme, the rotor relevitates quickly without unwanted dynamics.

Key words : AMB, Levitation, Recovery, Robust Control, Touchdown Bearing

1. Introduction

Industrially implementable AMB technology has been available for several years. However, utilization of AMBs in industry remains limited. This is due, largely, to the lack of familiarity with AMB technology among the body of practicing engineers. Subsequently, end users are resistant to purchase AMB systems for fear of the consequences of levitation failure. This work proposes an AMB control method which guarantees robust levitation recovery in the event of the acute loss of levitation.

Broadly speaking, there are two types of AMB failures, internal and external (Schweitzer and Maslen, 2009). Internal faults are those having to do with the components of the AMB itself. An example of an internal fault is a position sensor failure which would result in a severing of the feedback control loop and loss of levitation. The prevention of internal failures has been addressed by robustness of individual components and in certain cases, redundancy of components such as having more magnetic poles than is necessary. There has also been research on proper control of redundant AMB systems which are experiencing internal component failure (Maslen, et al., 1999).

External faults, conversely, are those which arise from factors outside of the AMB system. For example, a rotor supported on AMBs that processes natural material may encounter an aberration in the material consistency which exerts a onetime unsupportable load. The control solution proposed in this paper addresses the problem of external faults. In the event of an external fault, there is an acute loss of levitation and although there is no sustained component failures, recovery of levitation may be prevented by two phenomena. First, the fact that the rotor is outside of the specified operational limits may drive the control current into the saturation region (Khatri, et al., 2015). Saturation of control actuation is widely known to have adverse effects on stability. This issue is exacerbated by the coincidence of rotation forces. Second, shaft contact with the TD bearing while rotating may result in a so-called contact mode (Keogh and Cole, 2003). A contact mode is a nonlinear but stable mode of vibration of the rotor in contact with the TD bearing which is sustained by the motor feeding energy into the system. Different forms of contact modes are possible including forward whirl (continuous sliding), backward whirl (continuous rolling), and repeated impact (bouncing in a pattern). Whether and which type of contact mode occurs is determined by many factors such as orientation of the rotor, running speed, TD bearing friction (as well as stiffness and damping), unbalance, natural frequency, etc. The levitation recovery control method proposed and demonstrated in this work uses the model-based robust control strategy μ-synthesis. These two phenomena which may prevent relevitation when rotating are taken into account with the system model such that the synthesized control is robust to them.

Much of the existing body of literature in the area of control for relevitation addresses the synchronous disturbance due to TD bearing contact, e.g., (Cole and Keogh, 2003), (Abulrub, et al., 2006), and (Schlotter and Keogh, 2007). Therefore, algorithms similar to those for unbalance compensation are used. Good experimental results have been obtained using these approaches; however, a period of automatic disturbance learning is required which diminishes their practicality. There have also been efforts in the area of control of actuated TD bearings towards relevitation such as (Li, et al., 2012). More similar to the currently proposed method is (Khatri, et al., 2015) which implements a switching algorithm for a AMB controller manually tuned for levitation recovery of an industrial system.

The paper is structured as follows: Section 2 is a brief introduction to μ-synthesis robust controller design and explanation of how μ-synthesis is applied for a typical AMB at normal operating conditions and the proposed method of applying μ-synthesis for fault recovery. Then, Section 3 introduces the experimental test rig. Section 4 presents experimental results and simulation results of a drop test for the purpose of bounding the TD bearing forces which is used in fault recovery controller synthesis. Section 5 discusses details of the AMB controller design for the test rig for both normal operation and fault recovery. Section 6 is the experimental implementation of the proposed method and the comparison to using no recovery scheme. Finally, concluding remarks are made in Section 7.

2. μ-synthesis Controller Design for Normal Operation and Acute Fault Recovery

The controller design strategy μ-synthesis was developed to handle a system with structured uncertainties. The controller synthesis is carried out with an uncertain system model using the concepts of linear fractional transformation (LFT) and the structured singular value μ. These tools enable consideration of multiple uncertainties where they appear in the model, including the size and type of each uncertainty and how they interact. Therefore, a robust closed-loop can be designed which is not overly conservative which sacrifices performance.

The μ-synthesis problem formulation for a generalized system is shown in Fig. 1 A) where **P** is the plant, **K** is the controller, and **Δ** is the uncertain matrix. The structure of matrix **Δ** is a result of where each parametric uncertainty occurs in the system model. W_{in} and W_{out} are transfer function matrices which are chosen to specify the frequency dependent performance from the closed-loop system.

The matrix M is found as the lower LFT, F_l, of the weighted plant P' and the controller.

$$M = F_l(\mathbf{P}', \mathbf{K}) \tag{1}$$

The μ-synthesis framework is then cast with the upper LFT of the weighted closed-loop with the uncertainty perturbation which maps disturbance input w to performance response z.

$$z = F_u(M, \mathbf{\Delta})w \tag{2}$$

The smallest (in terms of maximum singular value) perturbation matrix Δ, belonging to the defined structure **Δ** and which destabilized the system M yields the so-called structured singular value μ from which μ-synthesis is named:

$$\mu(M) = \frac{1}{\inf\{\bar{\sigma}(\Delta):\det(I-M\Delta)=0, \Delta\in\mathbf{\Delta}\}} \tag{3}$$

The controller synthesis procedure seeks to find a controller by numerically iterating to minimize $\mu(M)$. If the resulting μ-value is less than one, it indicates that a greater than allowed uncertainty perturbation is required to destabilize the system. Therefore, the system closed-loop with the synthesized controller is stable and robust to the bounded uncertainties. For a derivation and thorough discussion of μ-synthesis, the reader is referred to the books by Zhou and Doyle (1998) and Skogestad and Postlethwaite (2005).

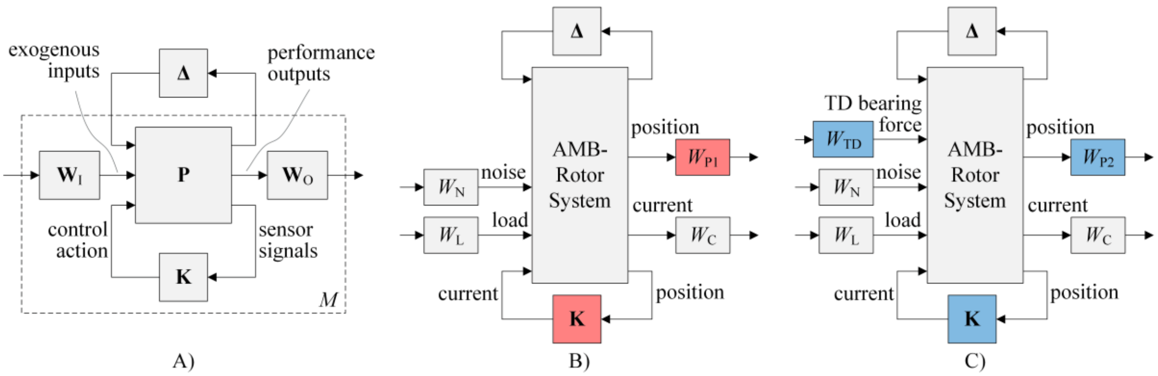

Fig. 1 A) Generalized μ-synthesis framework, B) basic μ-synthesis framework for normal operation AMB controller design, and C) μ-synthesis framework for robust fault recovery AMB controller design.

There are several specialized applications of μ-synthesis control for AMBs which take advantage of the model-based nature of μ-synthesis, such as for machining chatter attenuation (Pesch and Sawicki, 2012), machining tooltip tracking (Pesch, et al., 2015), and hydrodynamic bearing oil-whip stabilization (Pesch and Sawicki, 2015). However, for a basic AMB system, control is only concerned with providing stabilizing bearing stiffness in the presence of the flexible modes of the rotor and gyroscopic effect. Therefore, μ-synthesis for a basic AMB system is as follows and is illustrated in Fig. 1, plot B). The nominal plant to be controlled is the AMB-Rotor System. This consists of an FE model of the rotor, four radial AMB forces which are expressed linearly as current and position stiffnesses, and an amplifier model which quantifies the AMB slew-rate and delays due to digital implementation. The uncertainty perturbations account for AMB linearization errors and a varying running speed. An exogenous input and performance output are defined to achieve bearing stiffness and are load and position, respectively. The load is external load on the rotor at the AMB force center location and position is the rotor lateral deflection at the AMB sensor location. The weight on load W_L is designed to account for rotor weight at low frequency and unbalance load across the operational speed range and then roll off at high frequencies outside of the range of interest. The weight on position W_{P1} is crafted to require small deflection at low frequency and a practical orbit size across the operational speed range before rolling up at high frequency. The noise exogenous input is disturbance on the four sensor signals and is weighted accordingly. The current output is the control current. It is weighted with W_C which requires the controller response stay below the AMB bias current level and then rolls off as to not saturate the slew-rate. Earlier roll-off may be specified to prevent spillover effect where the controller excites rotor flexible modes that were neglected in the model.

The proposed μ-synthesis scheme for fault recovery is similar to that for basic AMB operation with two modifications. First, the weight on position performance is changed to allow for deflections up to the TD bearing clearance. Therefore, the resulting controller will not violate the AMB current limits in the event that the rotor should momentarily lose levitation. Second, an additional exogenous input is defined which accounts for any forces on the rotor due to contact with the TD bearings. The weight W_{TD} is selected to bound the magnitude of the TD bearing force at all frequencies and is robust to any phase angle by the nature of the μ criterion. This weighted input requires that the closed-loop system be stable in the presence of contact with the TD bearing.

For the remainder of this paper, the μ-controller designed for acceptable performance under normal operating conditions is be called the *performance controller* and μ-controller designed for robust fault recovery is called the *recovery controller*. The recovery controller, although stabilizing under extreme deflections, is not expected to yield bearing stiffness acceptable for healthy rotation. Therefore, a recovery scheme is proposed in which the performance controller is used until a delevitating event is detected at which point the AMB is automatically switched to the recovery controller. When the acute fault has passed, the AMB is automatically switched back to the performance controller after a prescribed time within an acceptable clearance limit.

3. Experimental Test Rig

The proposed fault recovery scheme is demonstrated on the experimental AMB test rig shown in Fig. 2. The test rig consists of a rotor supported on two radial AMBs and one thrust AMB. The TD bearings are rolling element type and are situated on the shaft directly outside of each radial AMB target rotor. The shaft diameter is 16 mm and the TD bearing radial clearance is 190 μm.

A) B)

Fig. 2 AMB test rig A) photograph, and B) basic dimensions. The test rig has a steel shaft supported by two radial AMBs and one thrust AMB manufactured by SKF. The rotor is driven by a DC electric motor via a flexible coupling. There is one disk between the bearings and each AMB has a target rotor. The TD bearings are rolling element type and are to the immediate outside of each radial AMB rotor.

The rotor is modeled with the FEM. FE nodes are placed at the AMB force and sensor locations for typical assembly of the open-loop plant model. FE nodes are also placed at the TD bearing locations for fault recovery controller synthesis. The open-loop plant is assembled including the FE rotor model, linear AMB model and PWM amplifier model. For more information on the test rig including parameters, modeling, and experimental identification, see (Pesch, et al., 2014).

4. Touchdown Bearing Force Estimation

The worst case TD bearing force on the rotor during failure must be bounded in order to synthesize the recovery controller which is required to be robust to that disturbance. A simulation is performed in order to estimate the TD bearing force. A simplistic TD bearing model is used in the simulation which is then tuned to match experimental time response data.

4.1 Drop Experiment and Simulation

The rotor is levitated and run at 2000 RPM. The current to the AMB coils is abruptly turned off and the rotor is allowed to fall freely onto the TD bearings while the motor is still driving rotation. Figure 3 shows the orbit response and time response from the outboard AMB sensor after the AMB support is removed. The rotor starts at the center of the AMB and then falls until it hits the TD bearing. The rotor bounces up and to the right due to the stiffness of the TD bearing and initial relative velocity between the TD bearing and rotor surface. After the initial bounce, the rotor rolls back and forth on the bottom of the TD bearing, driven by the motor and residual unbalance.

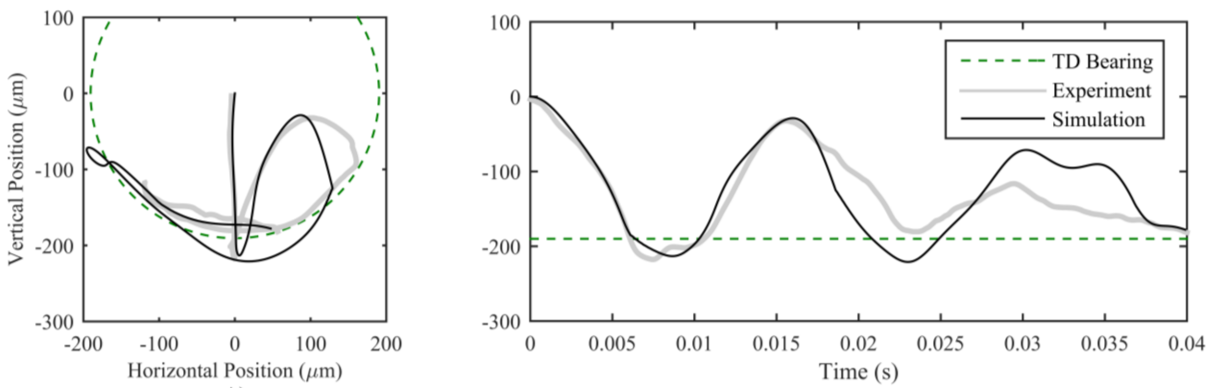

A) B)

Fig. 3 Response at outboard AMB sensor during 2000 RPM drop test, A) orbit, and B) time response. At 0 s, the rotor falls vertically downward until it makes contact with the TD bearing at which point it bounces driven by a normal force provided by the TD bearing stiffness and a tangential force provided by the relative velocity difference between the stationary TD bearing and the rotating shaft.

A numerical simulation of the rotor drop test is performed in MATLAB via *ode45*. The TD bearing is modeled as a discontinuous linear stiffness and damping. Also, an abrupt external force is applied at the moment of impact to account for initial difference between the rotor tangential velocity and the TD bearing. The parameters of the TD bearing and external force are manually tuned to match the data. The differences between the experiment and simulation are attributed to the simplicity of the TD bearing model. However, the similar magnitude of the overall response suggests that the simulated TD bearing force is of realistic magnitude. Therefore, the simple simulation is used as a practical solution to estimate the TD bearing force.

4.2 Simulated Touchdown Bearing Force Bounding

The simple TD bearing model with parameters tuned to the drop experiment is used in a simulation to bound the TD bearing force. The simulation includes a rotor drop impact followed by continuous running on the TD bearings for 10 s during which the rotor is driven by residual unbalance to bounce on the bottom of the TD bearings in a chaotic like fashion. For this time, the TD bearing forces in all four radial axes are collected. The frequency spectrum for the each of the four forces is found using FFT of the sampled numerical data. Then, for each frequency, the largest force from each of the four axes is taken. The result is the frequency spectrum shown in Fig. 4. The apparently noisy result is due to the chaotic like bouncing of the rotor on discontinuous stiffnesses and the frequency by frequency combination of the four axes forces. The TD bearing force is dominated by harmonics of the running speed, 1X, 2X, and 3X. Sidebands of the running speed harmonics and residuals from the natural frequencies are also present.

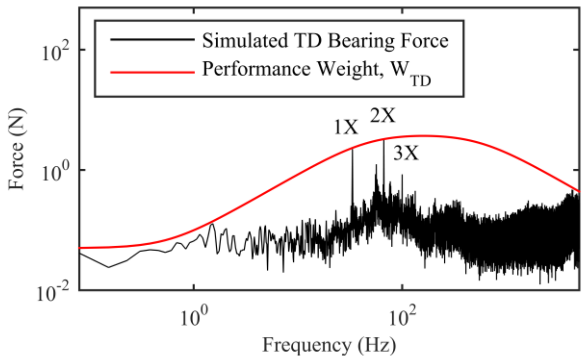

Fig. 4 Frequency spectrum of the simulated TD bearing force on the rotor and corresponding performance weighting function. The rotor rolling on the TD bearings exhibits highly chaotic behavior which is dominated by harmonics of the running speed and side bands. The TD forces from all four radial AMB axes are independently evaluated and the worst case (largest magnitude) force is taken for each frequency. The performance weight is tuned manually to bound the force on the rotor at all frequencies.

Figure 4 also shows the weighting function W_{TD}. W_{TD} is crafted manually to have greater magnitude than the simulated worst case TD bearing force at all frequencies. Then, W_{TD} is used to weight the exogenous perturbation input to the TD bearing FE node during controller synthesis. The transfer function of the final TD bearing force weight is presented in the next section on details of the experimental controller design.

5. Experimental Controller Design

5.1 Performance Specifications

The parametric uncertainties used for robust AMB controller are as follows and are summarized in Table 1. Uncertainties are placed on the two retained natural frequencies of the rotor model and on the current and position stiffness of the AMB to account for any mismatching between the nominal model and the system identification data. Uncertainty is placed on running speed which appears in the gyroscopic effect in the rotor model. The nominal running speed is set at 1000 RPM and a ±100% uncertainty covers the speed range from start up to target speed of 2000 RPM. The performance weights for mu-synthesis, with respect to the two control methods compared, are shown in Table 2.

Table 1 Parametric Uncertainties

Parameter	Type	Range
1st Natural Frequency*	Complex	±3%
2nd Natural Frequency*	Complex	±5%
Current Stiffness	Real	±5%
Position Stiffness	Real	±20%
Running Speed	Real	±100%

*Uncertainty placed on square of the natural frequency.

Table 2 Performance Weights

Signal	Weight	Units	Controller
Position	$W_{P1} = \frac{0.03125\,s+1.834}{s+16.5}$	μm^{-1}	Perf.
Position	$W_{P2} = \frac{2.632\times10^{-7}\,s+1.336}{s+253.9}$	μm^{-1}	Rec.
TD Force	$W_{TD} = \frac{1.382\times10^{4}\,s+5.052\times10^{4}}{s^2+3748\,s+1.01\times10^{6}}$	N	Rec.

Both performance controller and recovery controller have performance specifications for displacement at the AMB locations, W_{P1} and W_{P2}, respectively. The performance controller is required to hold the rotor in a small operating region while the recovery controller is allowed to deflect up to the TD bearing. The recovery controller is also required to withstand the force from the TD bearings onto the rotor, W_{TD}, which is discussed in the previous section.

5.2 Results of μ-synthesis for Operational Performance and Fault Recovery

μ-synthesis is performed on the two uncertain and weighted plant models using the MATLAB Robust Control Toolbox to perform the *D-K* iterations. The performance controller results from 2 *D-K* iterations achieving a μ-value of 0.89. The recovery controller results from 2 *D-K* iterations achieving a μ-value of 0.96. Therefore, each controller is expected to yield robust stability and robust performance for their corresponding operation regiments. Each controller is 4-input 4-output for each radial AMB axis. The Bode plots of one I/O pair on the main diagonal is shown in Fig. 5. This figure is for one axis of the outboard AMB and is characteristic of all main diagonal I/O pairs of the system.

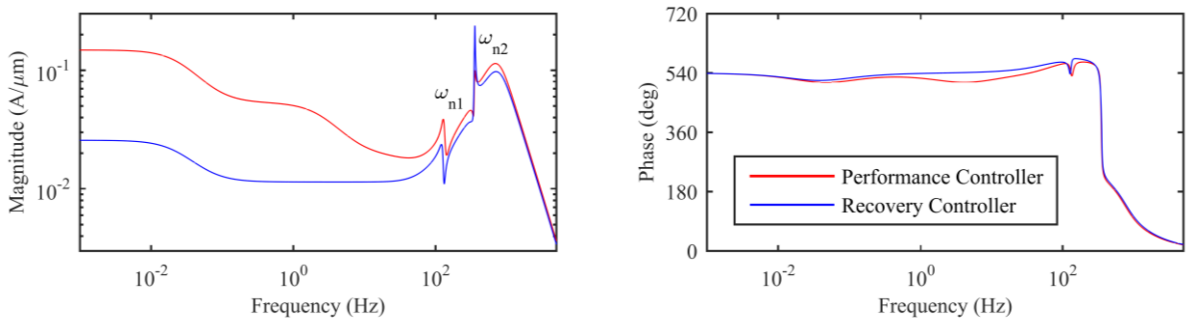

Fig. 5 Bode plot of AMB controllers designed through μ-synthesis. Both controllers exhibit an AMB stabilizing feedback and roll off at high frequency. The significant difference is the recovery controller has a much lower low frequency gain so as to mitigate coil saturation during large rotor displacements. Both controllers have features to compensate for the natural frequencies of the flexible rotor, ω_{n1} and ω_{n2}, however the performance controller is more aggressive on the first mode and the recovery controller more so on the second.

Both controllers exhibit negative feedback for stabilization of the AMBs. Both have features for control of the rotor flexible modes at ω_{n1} and ω_{n2} before rolling off at high frequency. The recovery controller has a significantly lower low frequency gain which prevents high control currents when the rotor is at large deflections such as would occur during loss of levitation. The recovery controller has lower gain at the first rotor mode but higher for the second.

6. Experimental Implementation

A switching scheme is utilized for implementation of the recovery controller (Cole, et al., 2004). The recovery controller replaces a typical AMB safety shutdown. If the rotor leaves a prescribed limit, the AMB switches to the recovery controller. The AMB then switches back after a prescribed time within the safety limit. To test the proposed recovery controller and switching scheme, an experiment is conducted. The test rig is levitated and rotated at 2000 RPM. Then, current to the AMB coils is abruptly stopped to mimic a power failure. The rotor is allowed to fall on to the TD bearings. After a time running on the TD bearings, the current is restored and the rotor relevitates while still rotating. Figure 6 shows the time history of the levitation failure and recovery test when using just the performance controller and the proposed recovery controller and switching scheme.

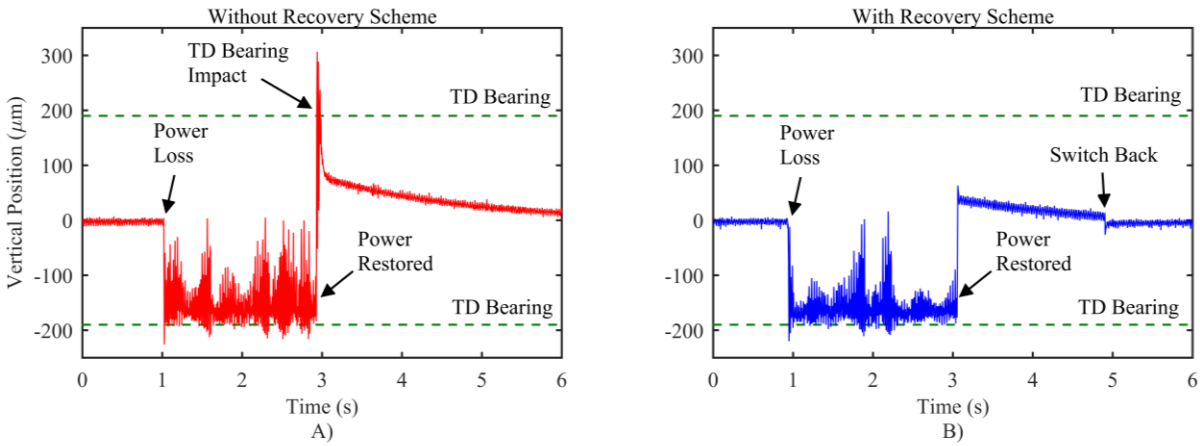

Fig. 6 Time responses in vertical direction at outboard AMB during 2000 RPM levitation failure and recovery test. Power to the AMB coils is stopped at approximately 1 s and restored at approximately 3 s. Plot A) uses no recovery scheme and results with an overshoot which hits the top of the TD bearing. Plot B) uses the proposed recovery controller which automatically triggers at -100 µm and responds with safe relevitation when power is restored. The system automatically switches back to the performance controller after approximately 2 s inside ±100 µm.

In each case, the rotor starts at the center of the AMB. At 1 s, the current to the AMB coils is stopped. The AMBs in the recovery trial are automatically switched from the performance controller to the recovery controller when the sensor signal surpasses predefined safety limit of ±100 µm. For both cases, from approximately 1 s to 3 s, the rotor runs supported only by the TD bearings resulting in chaotic like motion. At approximately 3 s, power is restored. The system with no recovery scheme responds violently with overshoot causing impact with the top of the TD bearing but it is ultimately able to return to stable levitation. The system with the recovery controller returns to stable levitation quickly with little unwanted dynamics. After approximately 2 s inside the ±100 µm safety limit, the AMBs automatically switch back to the performance controller. Figure 7 shows the corresponding orbit responses. Plots A) and B) show relevitation with the performance and recovery controllers, respectively.

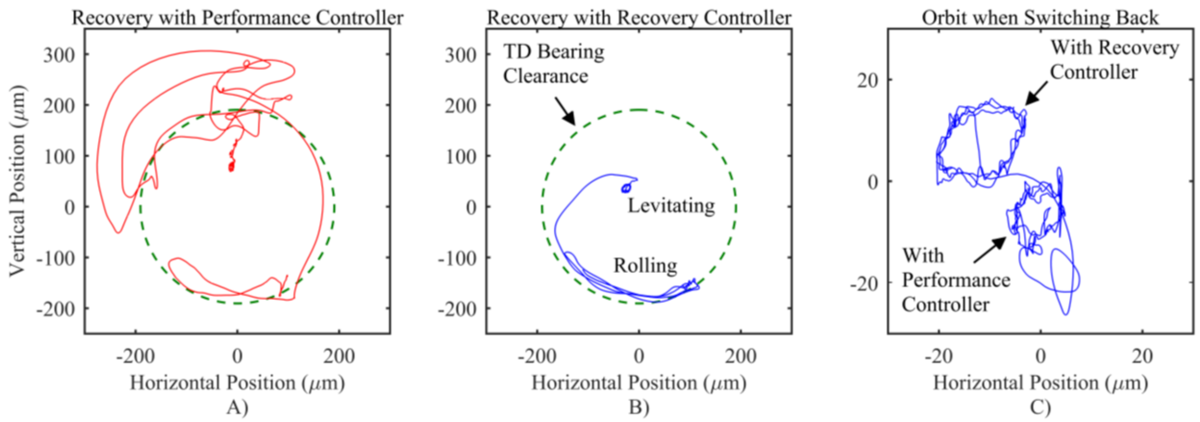

Fig. 7 Orbit at outboard AMB during 2000 RPM levitation recovery test. The circular dashed lines indicate the TD bearing radial clearance. Plot A) shows 0.2 s of data during recovery using the performance controller resulting in significant overshoot and touchdown bearing contact. Plot B) shows 0.2 s of data using the recovery controller resulting in quick and safe relevitation. Plot C) shows 0.2 s of data when automatically switching from the recovery controller back to the performance controller.

Plot C) shows the orbit of the recovery scheme trial when switching from the recovery controller back to the performance controller. Smaller orbit size and less overall deflection from the AMB center indicates superior performance of the performance controller when inside the proper operating region.

7. Conclusions

This paper proposed an AMB control method for relevitating a rotor which has been temporarily delevitated by an external fault. The proposed method uses μ-synthesis to design an AMB controller which is robust to very large rotor deflections and TD bearing forces on the rotor. The resulting recovery controller is automatically activated if rotor delevitation is detected.

The proposed levitation recovery method was demonstrated on an AMB test rig. The rig was run at 2000 RPM and the current to the magnetic coils was temporarily stopped to cause an external fault. After the rotor was running on the TD bearings, the power was restored. The trial using a baseline AMB controller responded violently, hitting the top of the TD bearing before recovering levitation. The trial using the proposed recovery controller was able to recover levitation quickly with no unwanted dynamics.

A deficiency in this work is the simplistic model used to estimate a bound on the TD bearing force used for controller design. Therefore, a direction of further research would be to apply this controller design method using a more sophisticated TD bearing model. Alternatively, experimentally gathered TD bearing force data may be used to create the performance bound.

References

Abulrub, A. G., Sahinkaya, M. N., Keogh, P. S. and Burrows, C. R., Experiments on ROLAC to recover rotor position following contact, Proceeding of the 10th International Symposium on Magnetic Bearings (ISMB10) (2006).

Cole, M. O. T. and Keogh, P. S., Rotor vibration with auxiliary bearing contact in magnetic bearing systems Part 2: robust synchronous control for rotor position recovery, Proceedings of the Institution of Mechanical Engineers Part C, Journal of Mechanical Engineering Science, Vol. 217 (2003), pp.393–409.

Cole, M. O. T., Keogh, P. S., Sahinkaya, M. N. and Burrows, C. R., Towards fault-tolerant active control of rotor-magnetic bearing systems, Control Engineering Practice, Vol. 12 (2004), pp.491–501.

Khatri, R. K., Hawkins, L. A. and Bazergui, C., Demonstrated operability and reliability improvements for a prototype high-speed rotary-disc atomizer supported on active magnetic bearings, Proceedings of ASME Turbo Expo 2015: Turbine Technical Conference and Exposition (2015), Paper No. GT2015-43803.

Li, P., Sahinkaya, M. N., and Keogh, P. S., Active Recovery of Contact-Free Levitation in Magnetic Bearing Systems, Proceedings of the ASME 2012 International Design Engineering Technical Conference & Computers and Information in Engineering Conference (2012), Paper No. DETC2012-70641.

Maslen, E. H., Sortore, C. K., Gillies, G. T., Williams, R. D., Fedigan, S. J., and Aimone, R. J., Fault Tolerant Magnetic Bearings, ASME Journal of Engineering for Gas Turbines and Power, vol. 121, issue 3, (1999), pp.504–508.

Pesch, A. H., Hanawalt, S. P., and Sawicki, J. T., A Case Study in Control Methods for Active Magnetic Bearings, Proceddings of the ASME Dynamic Systems and Control Conference (2014), paper no. DSCC2014-6257.

Pesch, A. H., Smirnov, A., Pyrhonen, O., and Sawicki, J. T., Magnetic Bearing Spindle Tool Tracking through μ-synthesis Robust Control, IEEE/ASME Transactions on Mechatronics, vol. 20, issue 3, (2015), pp.1448–1457.

Pesch, A. H., and Sawicki, J. T., Application of Robust Control to Chatter Attenuation for a High-Speed Machining Spindle on Active Magnetic Bearings, Proceedings of the 13th International Symposium on Magnetic Bearings (ISMB13), (2012).

Pesch, A. H., and Sawicki, J. T., Stabilizing Hydrodynamic Bearing Oil Whip with mu-synthesis Control of an Active Magnetic Bearing, Proceedings of the ASME Turbo Expo 2015: Turbine Technical Conference and Exposition (2015), paper no. GT2015-44059.

Schlotter, M. and Keogh, P. S., Synchronous position recovery control for flexible rotors in contact with auxiliary bearings, Transactions of the ASME, Journal of Vibration and Acoustics, Vol. 129, (2007), pp.550–558.

Schweitzer, G. and Maslen, E. H., Eds., Magnetic Bearings (2009), pp.407–433., Springer-Verlag.

Skogestad, S., and Postlethwaite, I., Multivariable Feedback Control: Analysis and Design (2005), Wiley.

Zhou, K., and Doyle, J. C., Essentials of Robust Control (1998), Prentice Hall.